Supplemental Fig 1

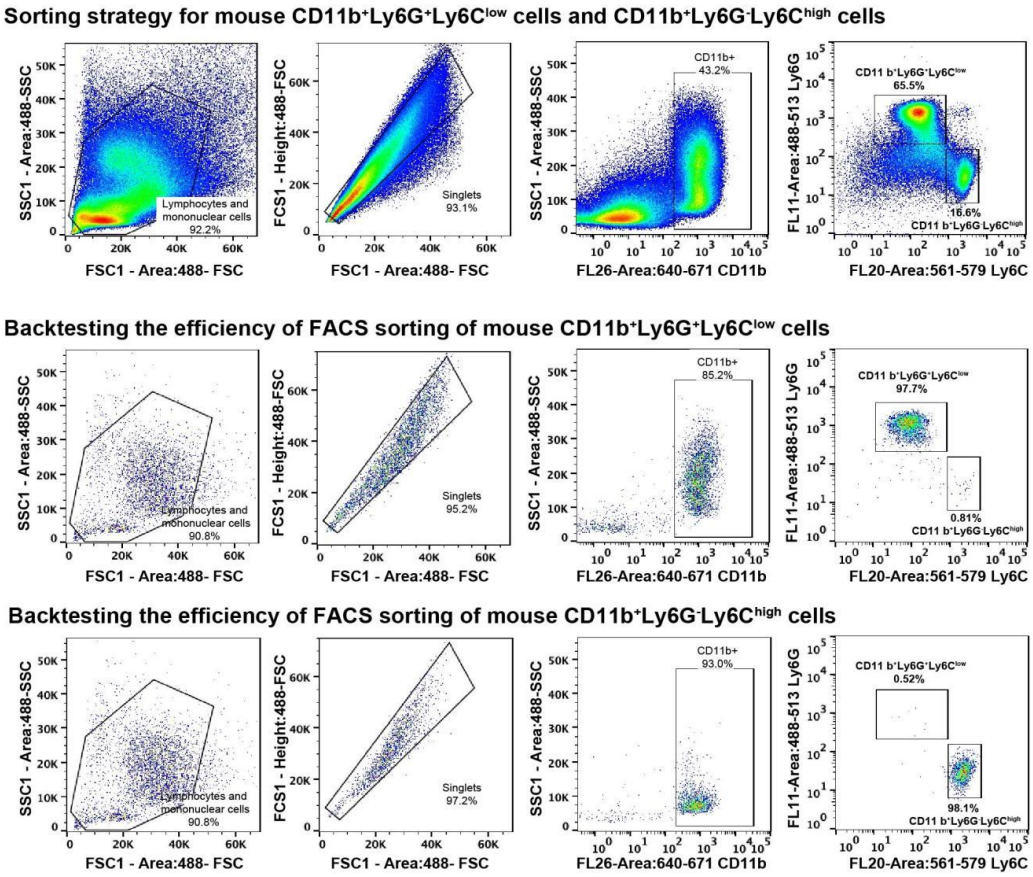

Gating strategy of $CD11b^{+}Ly6G^{+}Ly6C^{low}$ and $CD11b^{+}Ly6G^{-}Ly6C^{high}$ cells

FACS strategy to sort $CD11b^{+}Ly6G^{+}Ly6C^{low}$ cells and $CD11b^{+}Ly6G^{-}Ly6C^{high}$ cells derived from mouse bone marrow. Firstly, using FSC-A and SSC-A physical conditions to gate the lymphocytes and mononuclear cells; Secondly, adhesion cells were removed with FSC-A and FSC-H or FSC-W to get the single cell; Thirdly, $CD11b^{+}$ cells were gated by anti-mouse CD11b-APC and SSC-A parameters; Finally, using anti-mouse Ly6G-FITC and anti-mouse Ly6C-PE parameters to gate the target cells, respectively. According to the FACS sorting strategy, the purity of $CD11b^{+}Ly6G^{+}Ly6C^{low}$ cells reached 97.7% and the $CD11b^{+}Ly6G^{-}Ly6C^{high}$ cells is 98.1%.

Supplemental Fig 2

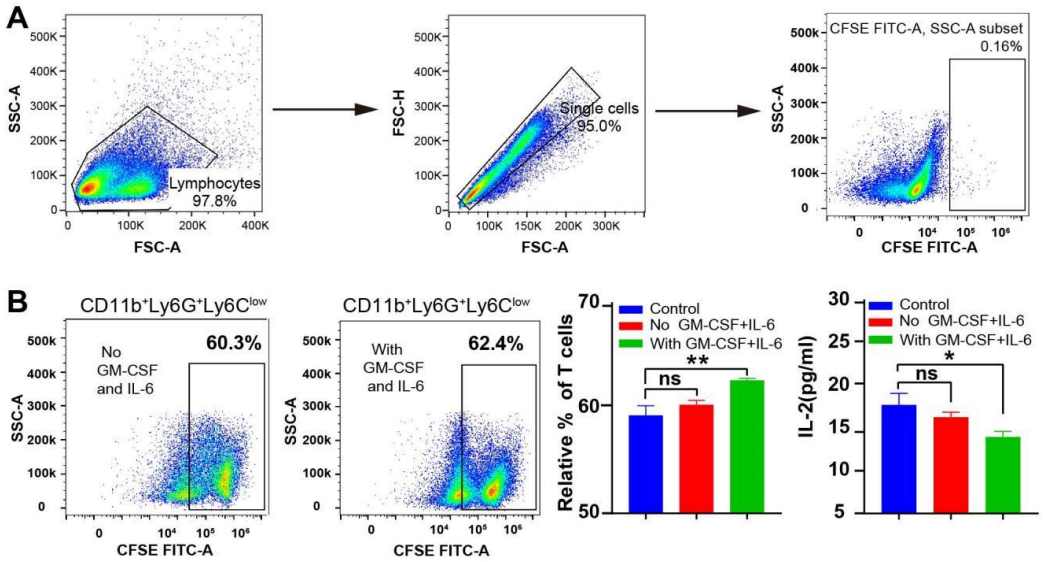

Effect of BM-derived CD11b^{+}Ly6G^{+}Ly6C^{low} cells on T cell proliferation

FCM analysis of the immunosuppressive ability of CD11b^{+}Ly6G^{+}Ly6C^{low} cells. **A**. Setting strategy to analyze T cell proliferation. Firstly, using FSC-A and SSC-A physical conditions to gate the lymphocytes cells; Secondly, gating the single cells by FSC-A and FSC-H parameters; Finally, testing T cell with CFSE at FITC panel. **B**. Assessment of the immunosuppressive ability of BM-derived CD11b^{+}Ly6G^{+}Ly6C^{low} cells. WT mice BM-derived CD11b^{+}Ly6G^{+}Ly6C^{low} cells cocultured with activated CFSE-labeled T cells without mouse GM-CSF and IL-6 stimulation as a naive group, cocultured cells with GM-CSF and IL-6 stimulation as a stimulation group, only activated CFSE-labeled T cells as a control, respectively. n =3. * P <0.05, ** P <0.01.

Supplemental Fig 3

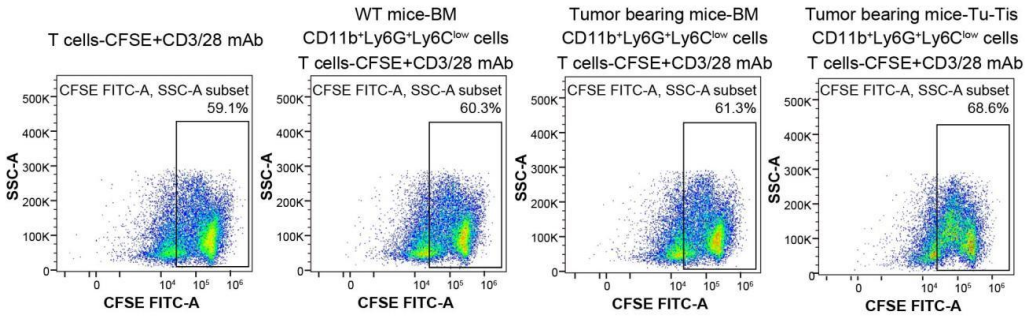

BM-derived CD11b^{+}Ly6G^{+}Ly6C^{low} cells from the tumor bearing mice suppress T cell proliferation

T cell proliferation were analyzed by FCM. We co-cultured activated CFSE-labelled T cells which were activated by anti-CD3 and anti-CD28 antibody with WT mouse BM-derived CD11b^{+}Ly6G^{+}Ly6C^{low} cells, tumor bearing mouse BM-derived CD11b^{+}Ly6G^{+}Ly6C^{low} cells and tumor tissue derived CD11b^{+}Ly6G^{+}Ly6C^{low} cells for 96 h, respectively. After that, the FITC signal intensity of T cells was detected by FCM.

Supplemental Fig 4

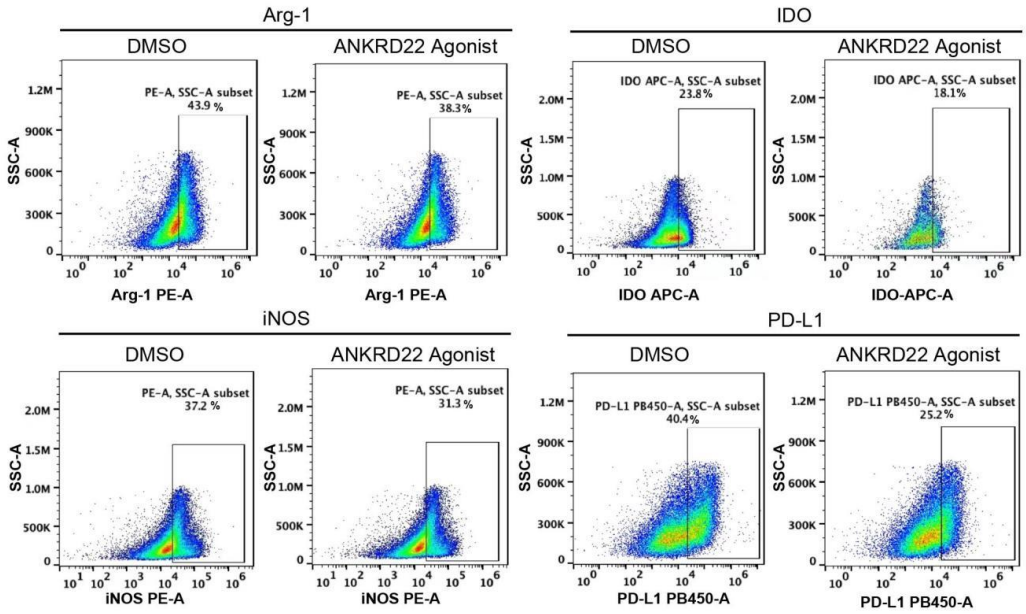

Effect of ANKRD22 agonist on immunosuppressive ability of PMN-MDSCs

PMN-MDSCs were treated with 1.0 μM ANKRD22 agonist for 72 h *in vitro*, and FCM showed the levels of Arg-1, iNOS, IDO and PD-L1 were reduced in PMN-MDSCs.

Supplemental Fig 5

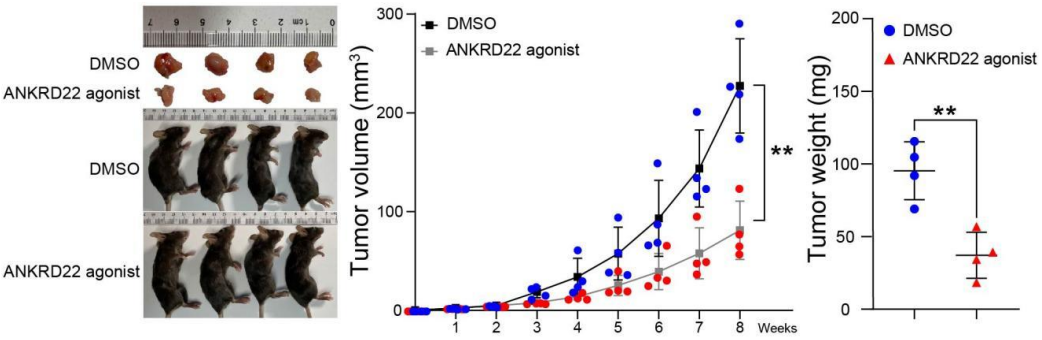

The immunosuppressive ability of PMN-MDSCs was reversed in transplanted tumor mouse models with treatment of an ANKRD22 agonist

PMN-MDSCs treated with 1.0 μM ANKRD22 agonist for 72 h and mouse ID8 ovarian cancer cells were mixed and suspended in Matrigel for subcutaneous tumorigenesis in C57BL/6 mice. Tumor diameters were measured with a Vernier caliper. n =4. ** P <0.01.

Supplementary Table 1

The clinical characteristics of patients

Parameters	Ovarian Ccancer Patients	Non-Ovarian Cancer Patients
Total number of cases	20	7
Age（years） Median (range)	58(42-74)	48(30-64)
Menopausal status		
Pre-	9	5
Post-	11	2
Ovarian involvement		
Unilateral	15	
Bilateral	4	
Tumor size		
＜10 cm	9	
≥10 cm	11	
FIGO stage		
I-III	7	
IV	13	
Residual tumor (TR)		
TR= 0 cm	5	
TR> 0 cm	15	
Presence of ascites		
Yes	9	
No	11	
Lymph nodes		
Negative	15	
Positive	5	
Platinum-based chemotherapy		
Yes	19	
No	1	
Histological type		
Non-epithelial	9	
Epithelial	11	
Grade		
Low	13	
High	7	
NLR		
<2.14	7	
≥2.14	13	
MLR		

	<0.24	5
	≥0.24	15
PLR		
	<146.11	5
	≥146.11	15